Journal of Engineering Science and Technology
Vol. 20, No. 3 (2025) 640 - 653

3D PRINTED WAVEGUIDE FILTER BASED ON SUPER-ELLIPTICAL SHAPE

WEI Y. SEE[1,*], SOEUNG. SOCHEATRA[1,*], SOVUTHY. CHEAB[2]

[1]Deapartment of Engineering, University Teknologi PETRONAS, Seri Iskandar Perak, 32610, Malaysia
[2]Institute of Digital Research & Innovation, Cambodia Academy of Digital Technology, Sangkat Prek Leap, Khan Chroy Changya, PhnoPenh, Cambodia
*Corresponding Author: wei_21000825@utp.edu.my

Abstract

This paper presents an approach to realize a 9th order super-ellipse waveguide filter applying circular inductive posts as the basic inductive discontinuity coupling technique. The super-ellipse waveguide overcomes the limitations of conventional rectangular waveguides using 3D metal printing, offering better flexibility in design. The application of shunt inductive posts eases the process of 3D metal printing, allowing it to be more accessible than other coupling methods. The filter design is formulated based on ninth-order Chebyshev polynomial, with the correlative characteristic polynomials and coupling matrix. Designed for a centre frequency of 22.85 GHz for 200 MHz bandwidth, this filter attains -15 dB minimum return loss and 1 dB insertion loss. The characteristic of narrowband frequency response allows the filter to be applied in various Radio Frequency, Microwave and Signal Processing application. The theory and experimental result show good agreement in the S-parameter response where centre frequency of 22.85 GHz and return loss of minimum -15 dB were achieved.

Keywords: Cavity resonator, Inductive post, Microwave filter, Waveguide, 3D-printing.

1. Introduction

With the development of 5G technology, the demand for microwave filters has increased rapidly. This increasing demand for microwave filters triggered sustainability awareness in the industry. Conventional CNC machining method are the most common fabrication method to fabricate microwave filters as it offers lower cost, but the low cost fabrication result in many materials wastage. While 3D printing allows the flexibility in design, speed in printing and wider choice of material.

There is an urgent need to design the microwave filter using 3D metal printing. Rectangular waveguide is the most common shape in microwave filter, but rectangular shape may have difficulty to be printed perfectly and require post processing due to the limitation of 3D metal printing. The rectangular shape still can be accepted but post processing will be required and it costly. Therefore, super-ellipse shape is proposed to solve this issue.

Waveguide filters are used to selectively pass or block signals at specific frequencies. Designing these filters comes with following challenges. The frequency stability and accuracy are crucial to achieve precise frequency responses is challenging, especially the filter require to maintain its performance across a series of conditions [1]. Any deviations in the design dimensions will significantly impact the filter's performance.

Ensuring that the fabrication process can achieve the expected tolerance is another significant challenge in this work. The requirement in precision in manufacturing waveguide filters is high as small deviations from the actual design will result in poor filter's performance. Therefore, the choice of coupling technique and manufacturing method are key to overcome such design challenges [2].

The application of 3D metal printing to fabricate rectangular cavities presents several challenges, due to the factors of uneven cooling and stress distribution. The sharp corners inherent in rectangular cavity designs may lead to problems like warping and layer separation during the 3D printing process. As proposed in [3], an alternative approach involves printing the rectangular cavity as two separate structures and joining the structure using screws. While this method is a viable solution, but the end results did not meet industry expectations and are open for improvement.

A major concern with this approach is the potential leakage at the joining parts using screws. In waveguide cavities, any minor uneven surface or leakage will significantly increase insertion loss, scattering losses of the electromagnetic waves and eventually result in poor waveguide performance. To overcome this problem, a super-ellipse shape is proposed. This shape offers great advantages in 3D printing, as it eliminates sharp angles and abrupt changes in direction, lowering the possibility of structural weakness and enhancing the overall printing process.

Recent studies on closed curved geometry cavities and 3D metal printing are attracting interest among researchers. In [3-5] it was shown that the application of closed curved geometry and 3D metal printing can achieve high performance as the rectangular waveguide. Most of the studies are applying iris opening to achieve resonator coupling because creating an opening in the waveguide cavity can be much more straightforward but the rough corner of the iris will impact the filter performance. Waveguide posts offer greater filter performance over irises as posts allow more precise control on the electromagnetic fields [6-9]. Posts can be designed and placed to control the resonant frequencies and achieve acute

frequency responses. Therefore, in this paper the circular inductive posts as the coupling technique are applied to compensate the setback of the iris coupling.

In this paper, super-ellipse waveguide with circular inductive post is designed and realized with 3D metal printing. Sec. 2 describes the theoretical formulation of the filter including the ninth-order filter, inductive post coupling and ninth-order filter. Sec. 3 presents the waveguide filter design and simulation, the waveguide design in software and important parameters are discussed. Sec. 4 shows the fabrication and measurement of the proposed filter. Simulated and measured filter responses are computed to provide verification on the proposed waveguide filter. Finally, Sec. 5 the paper conclusion is discussed. Overall, the highlight of the work is the filter realization approach using super-ellipse cavity to replace conventional rectangular cavity to achieve high performance filter characteristics with 3D metal printing fabrication.

2. Theory and Formation of Filter

The waveguide filter is realized based on the ninth order Chebyshev polynomial which serves as a guiding concept. Characteristic polynomials and the coupling matrix are derived through recurrence relation and filter function which are essential to the implementation of the filter. The following equations and formulas lay as the foundation framework for explaining the details of the filter formation. The theoretical frameworks of filter topology and super-ellipse cavities are presented and discussed in this section.

Figure 1 shows the steps to derive the ninth order Chebyshev coupling matrix by specifying the filter parameters such of the filter order and the cutoff frequency. Following by computing the Chebyshev polynomial using the recurrence relation. The explicit expression of ninth order Chebyshev polynomial is then used to derive the S-parameter transfer function. Construct the coupling matrix by organize the coupling coefficients into symmetric 9 × 9 matrix where the diagonal elements are the self-couplings, and the off-diagonal elements are the inter-moder couplings.

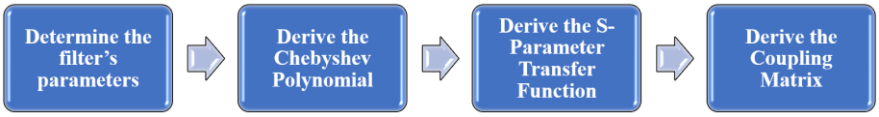

Fig. 1. The mathematical modelling flow of the Chebyshev Ninth Order.

2.1. Chebyshev nine order

There are plenty of applications for Chebyshev polynomials in filter designs. Chebyshev polynomials are applied in filter design to create filters with specific frequency response properties. The filter is designed based on the Chebyshev polynomial. The recurrence relation is used to derive the n-th Chebyshev polynomial for the first kind [10]:

$$T_{N+1}(\omega) = 2\omega T_N(\omega) - T_{N-1}(\omega) \quad (1)$$

where N is the order of the filter (initial condition).

$$T_{N+1}(\omega) = 1 \quad (2a)$$

$T_{N-1}$and (ω) = ω (2b)

So, the explicit expression for the ninth order Chebyshev polynomial $T_9(\omega)$ is:

$$T_9(\omega) = 256\omega^9 - 576\omega^7 + 432\omega^5 - 120\omega^3 + 9\omega \quad (3)$$

Furthermore, with the filtering function the S-parameter transfer function can be computed with the following expression [9]:

$$|S_{21}(j\omega)|^2 = \frac{1}{1+\varepsilon^2 T_N^2[\alpha\left(\frac{\lambda_g}{\lambda_0}\right)\sin\left(\pi\frac{\lambda_{g0}}{\lambda_g}\right)]}$$

$$|S_{11}(j\omega)|^2 = \frac{\varepsilon^2 T_N^2[\alpha\left(\frac{\lambda_g}{\lambda_0}\right)sin\left(\pi\frac{\lambda_{g0}}{\lambda_g}\right)]}{1+\varepsilon^2 T_N^2[\alpha\left(\frac{\lambda_g}{\lambda_0}\right)sin\left(\pi\frac{\lambda_{g0}}{\lambda_g}\right)]} \quad (4)$$

where λ_{g1} are the wavelengths of the upper band-edge.

λ_{g2} is the wavelength lower band-edge.

λ_g is the guided wavelength.

$\lambda_{g0} \approx (\lambda_{g1} + \lambda_{g2})/2$

Ɛ is the ripple level.

The design of the Chebyshev filter is formulated based on the Chebyshev polynomials, which are a series of orthogonal polynomials. A ninth-order Chebyshev filter, the filter design is based on the ninth degree of Chebyshev polynomial. The filter's order reflects the number of reactive components used in its design. The coupling matrix is a method used in the synthesis of the filter, it indicates the interactions between the different stages or the filter's components.

The coupling matrix for a ninth-order Chebyshev waveguide filter has dimensions of 9 × 9 corresponds to the filter's order. The coupling strength between the two resonant cavities is represented by the element of the matrix. A simplified example of ninth order coupling matrix:

$$\begin{matrix} 0 & k_{1,2} & 0 & 0 & 0 & 0 & 0 & 0 & 0 \\ k_{2,1} & 0 & k_{2,3} & 0 & 0 & 0 & 0 & 0 & 0 \\ 0 & k_{3,2} & 0 & k_{3,4} & 0 & 0 & 0 & 0 & 0 \\ 0 & 0 & k_{4,3} & 0 & k_{4,5} & 0 & 0 & 0 & 0 \\ 0 & 0 & 0 & k_{5,4} & 0 & k_{5,6} & 0 & 0 & 0 \\ 0 & 0 & 0 & 0 & k_{6,5} & 0 & k_{6,7} & 0 & 0 \\ 0 & 0 & 0 & 0 & 0 & k_{7,6} & 0 & k_{7,8} & 0 \\ 0 & 0 & 0 & 0 & 0 & 0 & k_{8,7} & 0 & k_{8,9} \\ 0 & 0 & 0 & 0 & 0 & 0 & 0 & k_{9,8} & 0 \end{matrix} \quad (5)$$

where $k_{i,j}$ represents the coupling strength between the i th and jth resonant cavities.

In the matrix, the non-zero entries $k_{i,j}$ indicates the coupling strength between the stages i th and jth. These are the values derived from the polynomial coefficients and the design specifications of the waveguide filter. Based on the Chebyshev polynomial of the ninth-order shown in Eq. (3), which is used to define the filter's frequency response, the final coupling matrix can be formulated as Eq. (7). The

coupling matrix rotation is applying a transformation to the coupling matrix to simplify the original matrix structure and allow the design easier to be implemented. By simplifying the coupling matrix, the design and implementation of the filter can become straightforward. Transforming a complex matrix into a diagonal or nearly diagonal form is much easier to analyse and design.

$$K_{i,j} = 2\left\lfloor \frac{1}{\omega_i - \omega_i} \right\rfloor \text{ for i}\neq\text{j} \tag{6}$$

where ω_i and ω_j represent the resonant frequencies of the i [th] and j[th] modes and $K_{i,j}$ is the coupling coefficient between them.

The final coupling matrix after rotations is computed and demonstrated as follows.

$$M = \begin{bmatrix} 0 & 1.082 & 0 & 0 & 0 & 0 & 0 & 0 & 0 & 0 & 0 \\ 1.082 & 0 & 0.902 & 0 & 0 & 0 & 0 & 0 & 0 & 0 & 0 \\ 0 & 0.902 & 0 & 0.614 & 0 & 0 & 0 & 0 & 0 & 0 & 0 \\ 0 & 0 & 0.614 & 0 & 0.564 & 0 & 0 & 0 & 0 & 0 & 0 \\ 0 & 0 & 0 & 0.564 & 0 & 0.549 & 0 & 0 & 0 & 0 & 0 \\ 0 & 0 & 0 & 0 & 0.549 & 0 & 0.549 & 0 & 0 & 0 & 0 \\ 0 & 0 & 0 & 0 & 0 & 0.549 & 0 & 0.564 & 0 & 0 & 0 \\ 0 & 0 & 0 & 00 & 0 & 0 & 0.564 & 0 & 0.614 & 0 & 00 \\ 0 & 0 & 0 & 0 & 0 & 0 & 0 & 0.614 & 0 & 0.902 & 0 \\ 0 & 0 & 0 & 0 & 0 & 0 & 0 & 00 & 0.902 & 0 & 1.082 \\ 0 & 0 & 0 & 0 & 0 & 0 & 0 & 0 & 0 & 1.082 & 0 \end{bmatrix} \tag{7}$$

The ninth-order inline inductive post waveguide filter is formulated and designed with the following specific design properties:

1. Centre frequency at 22.85 GHz.
2. Return loss of at least 15 dB within the passband.
3. Bandwidth of 200 MHz
4. Insertion loss lower than 1 dB.

The topology of the filter is synthesized, as shown in Fig. 2 where the shaded circles represent the resonator, and the unshaded circles represent the source and load. The shaded line shows the connection of the topology.

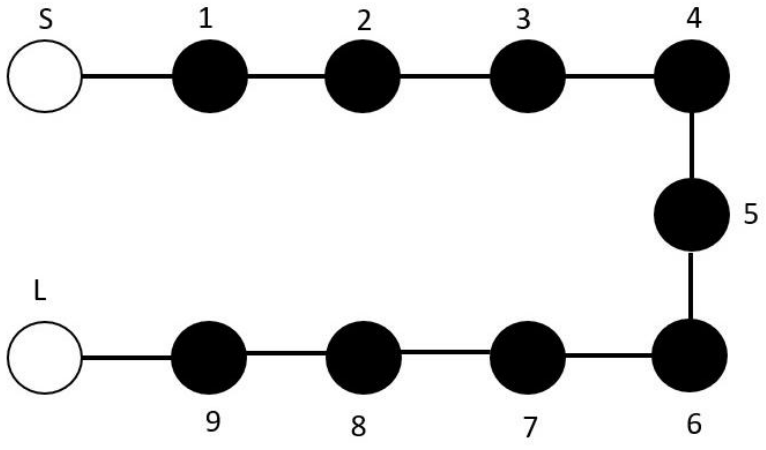

Fig. 2. Filter topology rerouting structure of the ninth order filter.

2.2. Resonator cavity

The total normal-force-curve slope of nose-cylinder-boattail body is determined by the summation of the normal-force-curve slopes of the nose (with the effect of cylindrical part) and afterbody.

A Super-ellipse also known as a Lame curve, is a closed curve similar to an ellipse, preserving the geometric features of semimajor axis and semiminor axis but a different overall shape. The generalized super-ellipse is defined by:

$$\left|\frac{x}{a}\right|^m + \left|\frac{y}{b}\right|^n = 1\,; m, n > 0 \tag{7a}$$

$$x(t) = |\cos t|^{\frac{2}{m}} \cdot asgn(\cos t) \tag{7b}$$

$$y(t) = |\sin t|^{\frac{2}{n}} \cdot bsgn(\sin t) \tag{7c}$$

Compared to the rectangular cavity, the super-ellipse cavity had higher performance for the same higher order resonances. However, this cavity is much more configurable as a filter by allowing the coupling structures to be more compact without needing the intersection with the cavity [3, 4]. It is thus shown that the cavity will improve the overall filter performance for a given far-out-of band response. The values of m = 4 and n = 5 are used in the formation of the super-ellipse in this work.

2.3. Realization of the proposed filter

The waveguide filter comprises a basic component as the cavity resonator, which use metallic hollow structures to manipulate electromagnetic waves. Electromagnetic signals trapped within the resonator are reflected back and forward between the source and load [6, 11]. In order to create the resonant modes which, resonate with the intended frequencies, these waveguide cavities are constructed with specific dimensions and configurations. These cavities are placed within the waveguide structure based on the calculation will allow certain frequencies to pass through and effectively filtering the signal by attenuating others.

The waveguide filter is designed in narrowband frequency response to meet several intended applications. The filter is designed to allow only a narrow range of frequencies and reject others. Narrowband filters can be used to minimizing interference from nearby frequency bands and improving the signal to noise ratio. Narrowband filters are important in bandwidth-limited system to improve bandwidth efficiency in microwave communication links allows efficient transmission without unnecessary use of spectrum. The ninth-order narrowband waveguide filter with hundreds of MHz bandwidth is designed to meet application in radar system, microwave, RF system, spectral analysis, signal processing, telecommunication and broadcasting.

Posts are one of the common elements found in cavity resonators that interfere the electromagnetic waves that pass from the two ends. The waveguide post is literally just a post that comprises a conductive material. An inductive post will extend and touch completely from the top through bottom walls. The effect an inductive post in rectangular waveguides and its advantage over an iris were discussed in [6, 8]. Therefore, in this paper, inductive posts are used as the coupling technique to design ninth order in-line waveguide filters.

Inductive coupling can be introduced using thin or thick iris. This paper, the idea of using circular inductive posts is proposed due to their smaller size advantage in comparison to thick iris and finer fabrication process compared to thin iris. The idea is to place inductive cylindrical posts parallel to the narrow wall within the waveguide cavity.

The impact of a single inductive post obstacle in waveguide was covered [12]. Multiple post-inductive obstacles were introduced in waveguides [13]. A productive technique for the design and analysis of waveguide bandpass filters with multiple inductive circular posts is proposed [14-16]. All of these findings were proposed in a rectangular waveguide.

In this work, shunt inductive posts are applied as a coupling technique for designing the in-line super-ellipse waveguide filters. The dimensions and location of the circular posts are calculated.

The post reactance [17] is given by,

$$X_{kj}\overline{(\omega)} = \overline{\omega}\sum_{m=0}^{N-1}\frac{r_{kj}{}^{(m)}}{1-(\frac{\overline{\omega}}{\overline{\omega_m}})^2},\ 1\leq k, j\leq n_a \tag{8}$$

where, N is the order of the filter (number of poles), r is the radius of inductive post.

MATLAB program is used to compute the parameters of the proposed design. Once the initial values are obtained, ANSYS HFSS is used to perform the 3-D simulation and optimization of the computed cavity.

3. Waveguide Filter Design and Simulation

Filter design of waveguide includes creating a filter within a waveguide cavity to guide the passing of specific frequencies. After determining the filter's specifications and filter type (Chebyshev), simulation is crucial in this process to analyse the expected filter performance. In this paper, ANSYS HFSS tool is utilized to design and simulate the waveguide model to predict the expected behaviour of the filter. Simulation can be used to refine the design, optimize performance, and assure the filter meets the proposed specification. The 3D structure layout of waveguide filter is shown and discussed in this section. The details of the structure layout such as the distribution of the layout, important parameters and waveguide opening are clearly listed and discussed to serve as references for future.

Waveguide is designed and simulated in ANSYS High Frequency Simulation Software (HFSS). Figure 3 shows the 3D structure layout of the waveguide filter. The waveguide consists of a source and load inductive post followed by 8 pairs of inline inductive posts. The distribution and important parameters of the inductive post are shown in Fig. 4 where L is the length of the waveguide, W is the width of the waveguide, L1-L5 is the distance between posts and S1-S4 is the distance between the respective pair.

Another important parameter is the waveguide opening, since the waveguide cavity was designed under the WR42 waveguide size that operates between 18 GHz and 26.50 GHz, with dimensions of a = 10.668 mm and b = 4.318 mm. The values of the design parameters of the three waveguides are listed in Table 1. The raw material of silver is chosen because it is a favourable conductor. Ninth order inductive post waveguide filter with parameters as shown in Fig. 5.

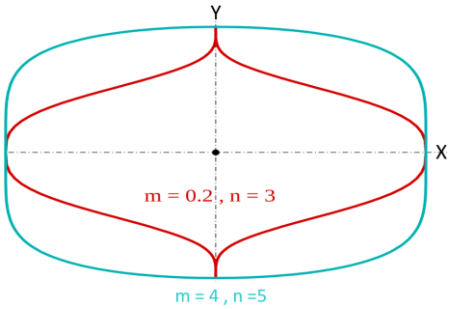

Fig. 3. The configuration of a super-ellipse with m and n values.

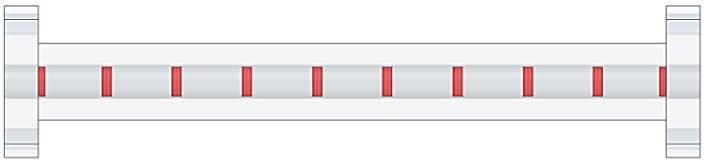

(a) Side view.

(b) Top view.

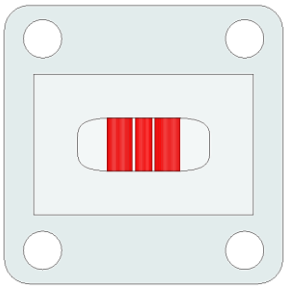

(c) Front view

Fig. 4. 3D structure layout of waveguide filter.

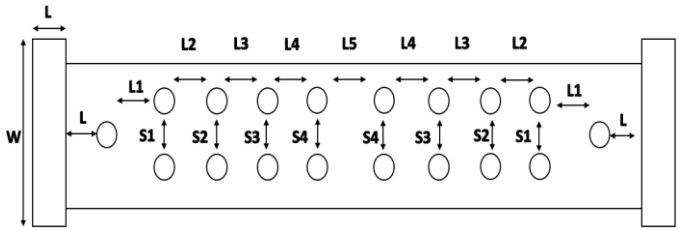

Fig. 5. Ninth order inductive post waveguide filter with parameters.

Table 1. Parameters of the waveguide.

Parameter	Super-ellipse
L(mm)	5
W(mm)	22.4
L1(mm)	7.3564
L2(mm)	7.8350
L3(mm)	7.8950
L4(mm)	7.9170
L5(mm)	7.9240
S1(mm)	2.2810
S2(mm)	1.9680
S3(mm)	1.8280
S4(mm)	1.7800

4. Fabrication and Measurements

Fabrication and measurements are important for research because they are crucial to validate the design, allow the theoretical modes to be validated and benchmarking against current standards. The super-ellipse waveguide is fabricated using the 3D printing method. The waveguide filter fabricated with the exact design geometry and parameters presented in Table 1. Post processing required after the waveguide filter printed using 3D metal printing as the surface roughness of the initial printing is higher than expected.

The initial prototype undergoes a series of post processing process of sanding and smoothing. This will help the protype to remove layer lines and uneven surface resulting in a smoother surface finish. Poor surface roughness in waveguide filter will result in poor filter performance by increasing the resistance of the waveguide wall, which reduces the efficiency of signal transmitting along the filter. At the same time, rough surface can cause deviations in the resonant frequency and Q factor of the waveguide filter. This may lead to the shifting of the cutoff frequency, which significantly result in poor filter's selectivity and overall performance. Therefore, minimizing surface roughness is important for achieving high filter performance. Side view of fabricated waveguide filter as shown in Fig. 6, and top view of fabricated waveguide filter as shown in Fig. 7.

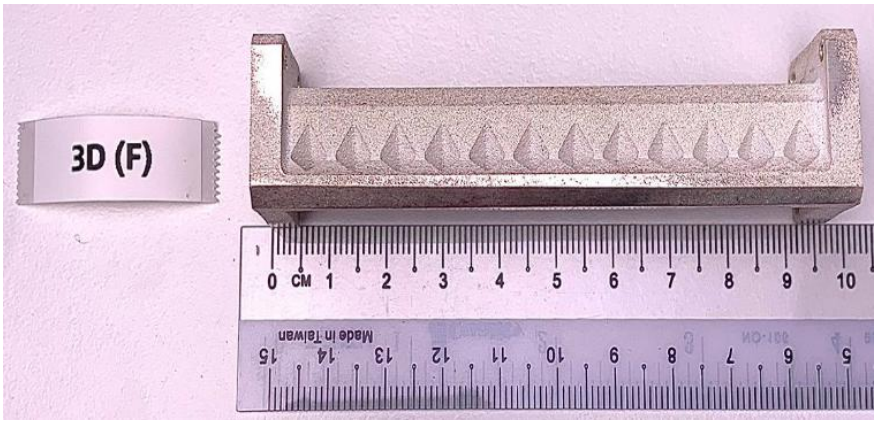

Fig. 6. Side view of fabricated waveguide filter.

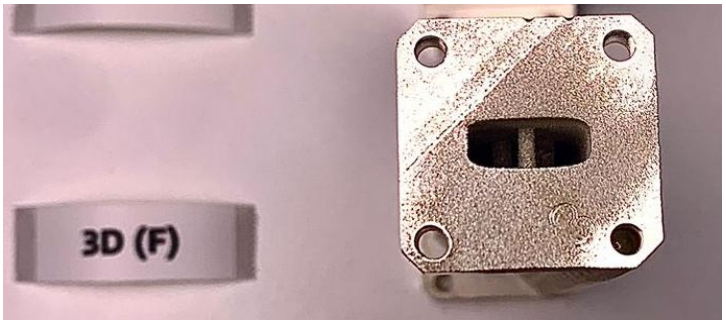

Fig. 7. Top view of fabricated waveguide filter.

The measurement of the prototype is done by vector network analyser, it's a powerful tool for characterizing the frequency response of a waveguide filter. Figure 8 shows that the prototype connected with a pair of WR-42 square launchers. Coaxial cables are connected to the launchers that will allow the measurement from the network analyser. Through network analyser, the S-parameters can be measured, which can provide information about the filter's transmission across a specific range of frequencies.

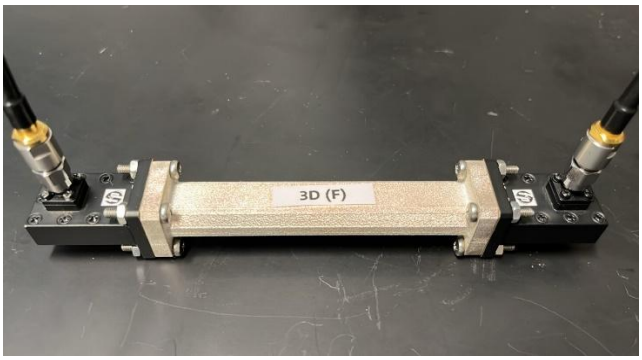

Fig. 8. Fabricated waveguide filter with WR42 launcher for measurement.

The designed filter matches the requirements mentioned in Section 2. It is designed to operate at the centre frequency of 22.85 GHz, with a return loss greater than -15 pp, bandwidth of 200 MHz and insertion loss of 0.1 dB. These parameters insertion loss, return loss, centre frequency and bandwidth are interrelated and important for ensuring the filter's performance, efficiency and suitability of the filter in different applications in radar, signal processing and communication system. The insertion loss is a crucial parameter that quantifies the amount of signal power loss as it propagates through the filter.

The return loss indicates the amount of signal that is rejected due to impedance mismatches. The centre frequency of a waveguide filter represent the frequency which the filter shows its peak transmission. It's important to precisely position the centre frequency at the desired point to allow filter effectively passes the desired signal and rejects the unwanted. The objective is to design the bandwidth at specific ranges is to match the specifications of the application. A narrow band of 200 MHz is suitable for selective filtering in communication and signal processing systems.

The measured and simulated S-parameter results of the waveguide filter for the prototype developed are shown in Fig. 9.

The actual measurements confirm the expected centre frequency as 22.85 GHz with a return loss of -18 dB, bandwidth of 200 MHz and an insertion loss of less than 1 dB. Both the simulated and measured results conform with the proposed filter specifications. Such difference may be as a result of the fabricated surface roughness of the prototype, which was found to be 2.0 microns (RA). This discrepancy may be lessened with an imitation of lower surface roughness.

Likewise further development on post-processing techniques will possibly allow surface roughness to below 1.0 micron (RA) and hence increase the S-parameter effectiveness of the filter. The variation between the simulated and measured results achieved a low variation based on the results shown in Fig. 9. The filter performance such as insertion loss and return also achieved as expected and met the standard requirements of the industry. Nonetheless, the fabricated filter validates this filter design based on super-ellipse cavity and the fabrication approach using 3D metal printing.

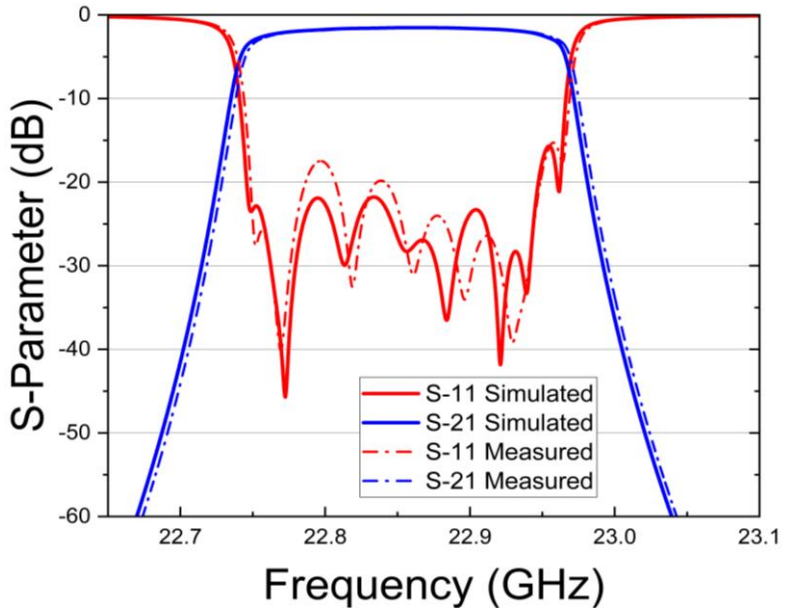

Fig. 9. Measured and simulated S-parameter of waveguide filter.

The technical contribution of the paper can be separated by different parts. One of the key contributions is the application of super-ellipse waveguide cavity to replace the conventional rectangular cavity. The application of complex cavity requires complex and accurate model of electromagnetic fields and interactions within the waveguide structure. Searching the optimal design parameters require various optimization techniques which are time consuming and computationally demanding. A set of optimal design parameters are shown and discussed in this paper. With the design parameters and the coupling techniques, another complex and high performance waveguide filter can be computed and designed. Comparative analysis of different filters as shown in Table 2.

Table 2. Comparative analysis of different filters.

Criterion	Proposed Filter	Filter 1 [4]	Filter 2 [12]
Frequency Response	Narrow Band	Narrow Band	Narrow Band
Insertion Loss	Low Insertion loss	Low Insertion loss	Low Insertion loss
Waveguide cavity	Super-ellipse	Super-ellipsoid	Rectangular
Coupling Method	Posts	Iris	Iris
Manufacturing Complexity	Complex	Moderate Complexity	Simple to manufacture
Return Loss	Average Return Loss -18 dB	Average Return Loss -18 dB	Lower return loss -22 dB
Fabrication Method	3D printed	3D printed	3D printed
Variation between simulation and measurement	Low	Medium	High

A comparative analysis of different filters was carried out to evaluate and compare more variables and options to identify differences and patterns. By assessing the filter characteristics, manufacturing method and filter performance to have better informed analysis. The selection of comparative filter is done based on same frequency response and fabrication methods with different waveguide cavity and coupling methods to explore and explain the similarities and differences of the filter performance.

All the filters and operating at narrow band frequency response and has a low insertion loss due to the characteristics of waveguide properties. The proposed filter used the posts as the coupling method while the rest used iris as the coupling method, which bring the manufacturing complexity of the proposed filter to complex. The filter 2 with rectangular waveguide cavity has a lower return loss around -22 dB but the variation between simulation and measurement is high.

While the proposed filter has an average return loss around -18 dB, the variation between simulation and measurement is low. Super-ellipse is a complex geometry closes to rectangular shape and eliminates the sharp corners of rectangular shape that will affect the overall filter performance caused by the poor finish at the corners. Based on the comparative analysis the proposed filter with complex manufacturing complexity compared to the rest but the variation between simulation and measurement is the lowest as well as meeting the basic filter performance.

5. Conclusions

This paper exemplified the capability of 3D printing to design based on super-elliptical shape. The super-elliptical shape shows the capability of achieving optimal filter performance and replacing the rectangular waveguide structures. The application of shunt inductive post makes easy for the 3D metal printing process and has similar performance to the other coupling methods. The measured results have a return loss of -18 dB which matches closely with the simulation results. Overall, the use of super-ellipse as waveguide cavity and shunt inductive post facilitates the 3D printing process that is more sustainable. In addition, a waveguide

based on super- elliptical shape is demonstrated here, to the best of our knowledge. This is the first in-line inductive post filter using super-elliptical cavity. The proposed technique can be applied for other elliptical high order filter designs. Future research may focus on further investigation of this type of super-ellipse cavities, including the design of high-order filter configurations, tunning screws and research into practical improvements in out-of-band rejection level.

Nomenclatures

$K_{i,j}$	Coupling Coefficient between i th and jth modes
$S_{11}(j\omega)$	S-parameter, input reflection coefficient
$\|S_{21}(j\omega)\|^2$	S-parameter, forward transmission coefficient
$T_9(\omega)$	Chebyshev polynomial of ninth order
X_{kj}	Post reactance

Greek Symbols

Ɛ	Ripple Level.
λ_g	Guided wavelength, m
(ω)	Angular Frequency

Abbreviations

3D	Three Dimension
5G	Fifth Generation
CNC	Computer Numerical Control
HFSS	High Frequency Simulation Software
WR	Waveguide Rectangular

References

1. Irum, L.; Sandhu, M.Y.; Lamecki, A.; Gomez-Garciaand, R.; and Mrozowski, M. (2024). Highly-compact dual-band bandpass waveguide filter based on cross-shaped frequency-dependent coupling. *Proceedings of the* 2024 *IEEE International Microwave Filter Workshop* (*IMFW*), Cocoa Beach, FL, USA, 140-142.
2. Mishra, G.K.; Pandey, H.K.; and Pathak, N.P. (2023). Substrate integrated waveguide filter based on inductive post design. *Proceedings of the* 2023 *IEEE Microwaves, Antennas, and Propagation Conference* (*MAPCON*), Ahmedabad, India, 1-4.
3. Tomassoni, C.; Peverini, O.A.; Venanzoni, G.; Addamo, G.; Paonessa, F.; and Virone, G. (2020). 3D printing of microwave and millimeter-wave filters: Additive manufacturing technologies applied in the development of high-performance filters with novel topologies. *IEEE Microwave Magazine*, 21(6), 24-45.
4. Booth, P.; and Lluch, E.V. (2017). Enhancing the performance of waveguide filters using additive manufacturing. *Proceedings of the IEEE*, 105(4), 613-619.
5. Martin-Iglesias, P.; van der Vorst, M.; Gumpinger, J.; and Ghidini, T. (2017). ESA's recent developments in the field of 3D-printed RF/microwave hardware. *Proceedings of the* 2017 11th *European Conference on Antennas and Propagation* (*EUCAP*), Paris, France, 553-557.
6. Martin, T.; Ghiotto, A.; Vuong, T.-P.; and Lotz, F. (2018). Fabrication-tolerant AFSIW filters based on quadruplet through-hole mounted inductive posts.

Proceedings of the 2018 48th *European Microwave Conference* (*EuMC*), Madrid, Spain, 749-752.

7. Darwish, M.M.; El-Tager, A.M.; Ahmed, H.N.; and El-Hennawy, H.S. (2008). Design of in-line dual-mode rectangular waveguide bandpass filters using multiple inductive circular posts. *Proceedings of the* 2008 38th *European Microwave Conference* (*EuMC*), Amsterdam, Netherlands, 500-503.
8. Hirokawa, J.; Sakurai, K.; Ando, M.; and Goto, N. (1990). A full-wave analysis of waveguide T-junction with an inductive post. *Proceedings of the International Symposium on Antennas and Propagation Society, Merging Technologies for the* 90*'s*, Dallas, TX, USA, 1250-1253.
9. Bhattacharjee, A.K.; Mukhopadhyay, A.K.; Kundu, J.; Mondal, B.; and Moitra, S. (2013). Substrate integrated waveguide (SIW) filter using stepped-inductive posts for KU-Band applications. *Proceedings of the Third International Conference on Computational Intelligence and Information Technology* (*CIIT*2013), Mumbai, India, 398-401.
10. Tan, J.M.; Cheab, S.; Ng, G.S.; and Soeung, S. (2021). Design & simulation of waveguide filter for 5G application. *Proceedings of the* 2020 8th *International Conference on Intelligent and Advanced Systems* (*ICIAS*), Kuching, Malaysia, 1-4.
11. Qi, L.; Xing, D.; Wang, R.; Qi, X.; and Zhao, J. (2020). Coupling matrix synthesis of general Chebyshev filters. *MATEC Web of Conferences*, 309, 01011.
12. Hunter, I.C.; Billonet, L.; Jarry, B.; and Guillon, P. (2002). Microwave filters-applications and technology. *IEEE Transactions on Microwave Theory and Techniques*, 50(3), 794-805.
13. Baranowski, M.; Balewski, Ł.; Lamecki, A.; and Mrozowski, M. (2023). Rectangular waveguide filters based on deformed dual-mode cavity resonators. *Proceedings of the* 2023 53rd *European Microwave Conference* (*EuMC*), Berlin, Germany, 400-403.
14. Mishra, G.K.; Pandey, H.K.; and Pathak, N.P. (2023). Substrate integrated waveguide filter based on inductive post design. *Proceedings of the* 2023 *IEEE Microwaves, Antennas, and Propagation Conference* (*MAPCON*), Ahmedabad, India, 1-4.
15. Ghazali, M.I.M.; Park, K.Y.; Gjokaj, V.; Kaur, A.; and Chahal, P. (2017). 3D printed metalized plastic waveguides for microwave *components. International Symposium on Microelectronics*, 2017(1), 000078-000082.
16. Teberio, F.; Arregui, I.; Gomez-Torrent, A.; Menargues, E.; Arnedo, I.; Chudzik, M.; Zedler, M.; Gortz, F.-J.; Jost, R.; Lopetegi, T.; and Laso, M.A.G. (2015). High-power waveguide low-pass filter with all-higher-order mode suppression over a wide-band for ka-band satellite applications. *IEEE Microwave and Wireless Components Letters*, 25(8), 511-513.
17. Zhu, L.; Rossuck, I.W.; Payapulli, R.; Shin, S.-H.; and Lucyszyn, S. (2023). 3-D printed W-Band waveguide twist with integrated filtering. *IEEE Microwave and Wireless Technology Letters*, 33(6), 659-662.